^{31}P NMR study of $Na_2CuP_2O_7$: an S = 1/2 two dimensional Heisenberg antiferromagnetic system

2006 J. Phys.: Condens. Matter 18 4285

(http://iopscience.iop.org/0953-8984/18/17/015)

INSTITUTE OF PHYSICS PUBLISHING JOURNAL OF PHYSICS: CONDENSED MATTER

J. Phys.: Condens. Matter **18** (2006) 4285–4294 doi:10.1088/0953-8984/18/17/015

^{31}P NMR study of $Na_2CuP_2O_7$: an $S = 1/2$ two dimensional Heisenberg antiferromagnetic system

R Nath[1], A V Mahajan[1], N Büttgen[2], C Kegler[2], J Hemberger[2] and A Loidl[2]

[1] Department of Physics, Indian Institute of Technology, Mumbai 400076, India
[2] Experimentalphysik V, Elektronische Korrelationen und Magnetismus, Institut für Physik, Universität Augsburg, D-86135 Augsburg, Germany

Received 31 January 2006
Published 13 April 2006
Online at stacks.iop.org/JPhysCM/18/4285

Abstract

The magnetic properties of $Na_2CuP_2O_7$ were investigated by means of ^{31}P nuclear magnetic resonance (NMR), magnetic susceptibility, and heat capacity measurements. We report the ^{31}P NMR shift, the spin–lattice ($1/T_1$), and spin–spin ($1/T_2$) relaxation rate data as a function of temperature T. The temperature dependence of the NMR shift $K(T)$ is well described by the $S = 1/2$ square lattice Heisenberg antiferromagnetic model with an intraplanar exchange of $J/k_B \simeq 18 \pm 2$ K and a hyperfine coupling $A = 3533 \pm 185$ Oe/μ_B. The ^{31}P NMR spectrum was found to broaden abruptly below $T \sim 10$ K, signifying some kind of transition. However, no anomaly was noticed in the bulk susceptibility data down to 1.8 K. The heat capacity appears to have a weak maximum around 10 K. With decrease in temperature, the spin–lattice relaxation rate $1/T_1$ decreases monotonically and appears to agree well with the high temperature series expansion expression for a $S = 1/2$ 2D square lattice.

(Some figures in this article are in colour only in the electronic version)

1. Introduction

Low dimensional spin systems with antiferromagnetic interactions have received considerable attention because of pronounced quantum mechanical effects which result in magnetic properties which are quite different from those of the three dimensional (3D) antiferromagnetic substances. According to the Hohenberg–Mermin–Wagner theorem [1], one dimensional (1D) and two dimensional (2D) spin systems with Heisenberg interaction and finite-range coupling between spins cannot have long range order (LRO) at any temperature different from zero. In 1D systems it does not occur even at zero temperature. However for 2D systems at zero temperature, LRO is not forbidden by this theorem. In fact, LRO has been rigorously established for spin $S > 1/2$, on a square lattice with nearest-neighbour coupling [2, 3]. For

the case of $S = 1/2$, there is no solid proof but there are strong theoretical arguments that LRO exists [4, 5].

The case of a $S = 1/2$ system on a square lattice, with nearest-neighbour antiferromagnetic coupling, has been of special interest because of its proximity to the high T_c cuprates. The interest in quasi-1D spin systems has been stimulated by the hope that better understanding of 1D systems might lead to insights into the 2D systems and high temperature superconductivity.

Already, a large number of $S = 1/2$ compounds have been experimentally investigated, which could be effectively described by 2D Heisenberg antiferromagnetic (HAF) models. Among the important ones are cuprate compounds such as La_2CuO_4 and $YBa_2Cu_3O_6$ which have CuO planes [6–8]. In La_2CuO_4, the intraplanar exchange coupling J/k_B was reported to be 1800 K. In spite of a small interplanar coupling $J' \approx 10^{-5}J$, the large correlations in CuO planes lead to 3D magnetic order at the Néel temperature $T_N \sim 300$ K. In the above cases T_N is strongly dependent on the J'/J ratio.

Most recently, $KCuF_3$ has been experimentally investigated as one of the quasi-1D HAF compounds [9, 10]. Unfortunately, this material has a relatively large coupling ratio $J'/J \sim 1.0 \times 10^{-2}$, due to which the T_N/J ratio (∼39 K/203 K) was found to be large. Later Sr_2CuO_3 was reported to be another 1D HAF system [11], with a significantly reduced T_N/J ratio of ∼5 K/2200 K $\sim 2 \times 10^{-3}$. Due to the relatively small T_N value compared to the exchange coupling J/k_B, 1D behaviour is observed over a wide range of temperature. Recently, Nath *et al* [12] have reported that $Sr_2Cu(PO_4)_2$ and $Ba_2Cu(PO_4)_2$ are two 1D HAF systems which do not appear to undergo Néel ordering even at a very low temperature ($T \sim 0.02$ K). Their exchange coupling constants have been reported to be 165, and 151 K respectively. It is thus of interest to synthesize and characterize additional $S = 1/2$ 1D or 2D HAF compounds to improve our understanding of such systems. In this paper, we present a detailed study of the magnetic properties of $Na_2CuP_2O_7$ via susceptibility and ^{31}P nuclear magnetic resonance (NMR) experiments. Our objective is to report detailed magnetic measurements on a new potentially low dimensional system and to analyse the data on the basis of available models. An additional objective is then to motivate the theorists to model real (and more complex) systems such as the ones we report and compare the results of their simulations with our data. Our results indicate that the magnetic properties of $Na_2CuP_2O_7$ agree with the 2D square lattice $S = 1/2$ HAF model somewhat better than the 1D model. In the next section, an overview of the schematic structure which motivated us to work on this system is presented. This is followed by details of our experiments. The 'experimental details' section is followed by results of our magnetic and heat capacity measurements, accompanied by an analysis and a conclusion.

2. Structure

The structural properties of $Na_2CuP_2O_7$ have been reported by Etheredge *et al* [13] and Erragh *et al* [14]. Its high temperature phase crystallizes in a monoclinic unit cell with space group $C_{2/c}$. The reported lattice constants are 14.715, 5.704, and 8.066 Å respectively along *a*-, *b*-, and *c*-directions. From the schematic diagram of the structure shown in figures 1(a) and (b), it is seen that the exchange interaction between Cu^{2+} ions could arise due to two interaction paths. (i) Each CuO_6 octahedron shares its corners with two similar kinds of PO_4 groups. The corner sharing takes place in one direction forming $[Cu(PO_4)_2]_\infty$ chains along the *c*-direction and in this case the magnetic properties would be those of a 1D HAF chain. (ii) Alternatively, there exist (nearly) 180° Cu–O–Cu linkages in the *bc* plane. Depending on the orientation of the $d_{x^2-y^2}$ orbitals (i.e. whether they are perpendicular to the *bc* plane or in the *bc* plane), the system will behave either as a chain-like or a planar magnetic system. In the latter case, however, one should note that the Cu^{2+} ions are arranged in a face centred manner

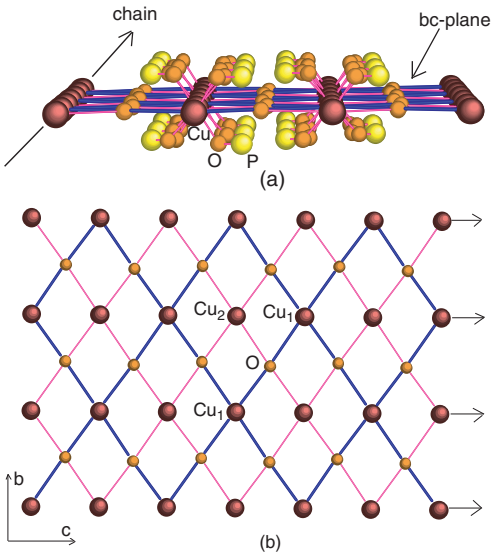

Figure 1. (a) A schematic diagram of the *bc* plane in $Na_2CuP_2O_7$ with $[Cu(PO_4)_2]_\infty$ linear chains propagating along the *c*-direction indicated. A possible coupling path Cu–O–P–O–Cu is also indicated. (b) The arrangement of Cu and O in the *bc* plane is shown. Two planes formed by Cu_1^{2+} and Cu_2^{2+} ions are represented by thick and thin bonds respectively.

(see figure 1(b)). One can, therefore, think of the *bc* plane as comprising two subplanes (shown in figure 1(b) by thick and thin lines). While the Cu_1–O–Cu_1 (or Cu_2–O–Cu_2) bond angle is almost 180°, the Cu_1–O–Cu_2 bond angle is somewhat less than 90°. The deviation of the magnetic properties of $Na_2CuP_2O_7$ from the square planar case would depend on the relative strength of the Cu_1–O–Cu_2 interaction, with respect to that of the Cu_1–O–Cu_1 (or Cu_2–O–Cu_2) interaction. Further, the interaction between the *bc* planes is expected to be weak since the distance between them is about 8 Å which is nearly twice the Cu^{2+}–Cu^{2+} intraplanar distance of 4 Å. Also, unlike the 180° Cu_1–O–Cu_1 intraplanar bonds case, there appear to be no similar interaction paths perpendicular to the *bc* plane.

3. Experimental details

A polycrystalline sample of $Na_2CuP_2O_7$ was prepared by solid state reaction technique using $NaH_2PO_4{\cdot}H_2O$ (98% pure) and CuO (99.99% pure) as starting materials. The stoichiometric mixtures were fired at 800 °C for 120 h, in air, with several intermediate grindings and pelletization. Formation of a nearly single phase sample was confirmed from x-ray diffraction, which was performed with a Philips Xpert-Pro powder diffractometer. A Cu target was used in the diffractometer with $\lambda_{av} = 1.541\,82$ Å. An impurity phase was identified as $Na_3P_3O_9$ and the intensity ratio (I_{imp}/I_{max}) was found to be 0.05, where I_{imp} is the intensity of the most intense diffraction peak for $Na_3P_3O_9$ and I_{max} is that of $Na_2CuP_2O_7$. Lattice parameters were calculated using a least-squares fit procedure. The lattice constants obtained are 14.703 (4) Å, 5.699 (2) Å, and 8.061 (3) Å, respectively along *a*-, *b*-, and *c*-directions. These are in agreement with previously reported values. Magnetization (M) data were measured as a function of temperature T (1.8 K $\leqslant T \leqslant$ 400 K) and applied field H (0 kG $\leqslant H \leqslant$ 50 kG) using a SQUID magnetometer (Quantum Design). The heat capacity was measured with a PPMS set-up (Quantum Design). The NMR measurements were carried out using pulsed

NMR techniques on ^{31}P nuclei (nuclear spin $I = 1/2$ and gyromagnetic ratio $\gamma/2\pi = 17.237$ MHz T^{-1}) in a temperature range 2 K $\leqslant T \leqslant$ 300 K using a ^{4}He cryostat (Oxford Instruments). We have done the measurements in an applied field of about 55 kG, which corresponds to a radio frequency (rf) of about 95 MHz. Spectra were obtained by plotting the echo integral (following a $\pi/2-\pi$ pulse sequence with a $\pi/2$ pulse of width 4 μs) as a function of the field at a constant frequency of 95 MHz. The NMR shift $K(T) = [H_{\rm ref} - H(T)]/H(T)$ was determined by measuring the resonance field of the sample ($H(T)$) with respect to that for a reference H_3PO_4 solution (resonance field $H_{\rm ref}$). The ^{31}P nuclear spin–lattice relaxation rate ($1/T_1$) was determined by the inversion–recovery method. The nuclear spin–spin relaxation rate ($1/T_2$) was obtained by measuring the decay of the transverse nuclear magnetization with a variable spacing between the $\pi/2$ and the π pulses.

4. Results and discussion

We first present the results of our ^{31}P NMR measurements on $Na_2CuP_2O_7$. Since there is a unique ^{31}P site, the ^{31}P NMR spectra consist of a single spectral line at high temperatures ($T \geqslant 5$ K) as is expected for $I = 1/2$ nuclei. The observed peak position shifts with respect to $H_{\rm ref}$ in the field sweep spectra. The temperature dependence of the ^{31}P NMR shift apparently arises due to the temperature dependence of the spin susceptibility $\chi_{\rm spin}(T)$ via a hyperfine coupling to the Cu^{2+} ions. The NMR shift is not affected by small amounts of extrinsic paramagnetic impurities whereas in the bulk susceptibility they give rise to Curie terms. NMR shift data as a function of temperature are shown in figure 2, for 5 K $\leqslant T \leqslant$ 300 K. They exhibit a broad maximum at 20 K, indicative of short range ordering. As explained earlier, the dominant magnetic behaviour of $Na_2CuP_2O_7$ could be that of a HAF chain or a plane. Consequently, we tested both the 2D (planar) and 1D (chain) models to fit the NMR shift data. A high temperature ($\frac{k_BT}{J} \gtrsim 0.7$) series expansion for the inverse susceptibility $1/\chi_{\rm spin}(T)$ for the 2D $S = 1/2$ HAF square lattice was given by Rushbrooke and Wood [15], which has the form

$$1/\chi_{\rm spin}(T) = \frac{J}{N_A\mu_B^2 g^2}\left[4x + \sum_{n=1}^{6}\frac{C_n}{(\frac{4}{3}x)^{n-1}}\right] \tag{1}$$

where $x = \frac{k_BT}{J}$, g is the Landé g-factor, μ_B is the Bohr magneton, N_A is the Avogadro number, and C_n are the coefficients listed in table 1 of [13]. Similarly Johnston [16] parametrized the low temperature ($\frac{k_BT}{J} \leqslant 1$) simulations of Takahashi [17] and Makivic and Ding [18] to obtain

$$\chi_{\rm spin}(T) = \frac{N_A\mu_B^2 g^2}{J}\big[0.043\,669 + 0.039\,566x - 0.5341x^3 + 4.684x^4 - 11.13x^5 + 10.55x^6 - 3.56x^7\big]. \tag{2}$$

For 1D HAF chains, the temperature dependence of the susceptibility $\chi_{\rm spin}(T)$ was numerically calculated by Bonner and Fisher [19]; the susceptibility for high temperatures was accurately predicted ($\frac{k_BT}{J} \geqslant 0.5$). Below, we use the form as given by Estes *et al* [20]:

$$\chi_{\rm spin}(T) = \frac{Ng^2\mu_B^2}{k_Bx} \times \frac{\big(0.25 + 0.074\,975x^{-1} + 0.075\,235x^{-2}\big)}{\big(1 + 0.9931x^{-1} + 0.172\,135x^{-2} + 0.757\,825x^{-3}\big)}. \tag{3}$$

Since the temperature dependence of the $\chi_{\rm spin}(T)$ is reflected in the NMR shift $K(T)$, one can determine the exchange coupling J/k_B and the hyperfine interaction A simultaneously by fitting the temperature dependence of K to the following equation:

$$K(T) = K_0 + \left(\frac{A}{N_A\mu_B}\right)\chi_{\rm spin}(T) \tag{4}$$

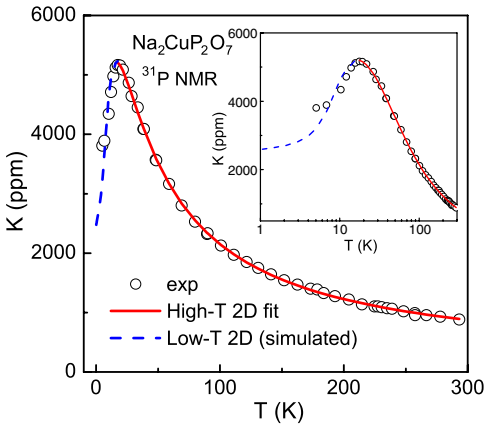

Figure 2. ^{31}P NMR shift K versus temperature T for $Na_2CuP_2O_7$. The solid line is a fit to equation (4) over the temperature range, 15 K $\leqslant T \leqslant$ 300 K, where χ_{spin} is the high temperature series expansion for susceptibility of the HAF square plane (equation (1)). The dashed line is the simulated curve from equation (2), with the parameters obtained from the high T fit. In the inset we have displayed the data at low temperatures on a logarithmic scale in order to show the deviation of experimental data from the low T series expansion.

Table 1. Values of the parameters obtained from the fitting of NMR shift to equation (4) considering 2D square planar HAF (equation (1)) and 1D HAF (equation (3)) models.

	K_0 (ppm)	A (Oe/μ_B)	$\frac{J}{k_B}$ (K)
Figure 2	100 ± 50	3533 ± 185	18 ± 2
Figure 3	143 ± 60	3479 ± 200	28 ± 5

where K_0 is the chemical shift. Figures 2 and 3 show fitting of the ^{31}P NMR shift data to equation (4) taking χ_{spin} for the HAF square lattice (equation (1)) and linear chain (equation (3)) respectively. In figure 2, the fitting to the 2D high temperature series expansion was done for 15 K $\leqslant T \leqslant$ 300 K, whereas in figure 3, the experimental data were fitted to the linear chain model in the temperature range 5 K $\leqslant T \leqslant$ 300 K. The parameters extracted from the fit are listed in table 1. The Landé g-value was found to be $g = 2.1$, which is a typical value for cuprates.

From figures 2 and 3 it is seen that our $K(T)$ data fit somewhat better to the 2D HAF model. At low temperature ($T \leqslant 25$ K), the 1D fit deviates from the experimental data. In figure 2, we have also plotted the simulated low temperature curve using equations (2) and (4) with the parameters K_0, A, and J/k_B obtained from the high temperature fit along with our experimental data. It is clearly seen that our experimental data do not deviate significantly from the simulated curve down to $T \sim 10$ K while a large deviation is seen below 10 K. This suggests some transition or crossover below 10 K.

An observation of the ^{31}P NMR lineshapes below 10 K (shown in figure 4) reveals a huge broadening at lower temperatures. Further, the lineshape develops shoulder-like features and finally at 2 K the overall extent of the spectrum is about five times that at 10 K, with at least three distinct peaks. Either a structural or a magnetic transition might be the cause for this. No anomaly is seen in the bulk susceptibility (see below) which seems to go against the occurrence of 3D LRO.

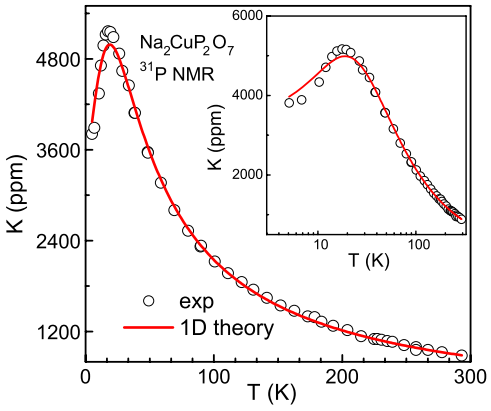

Figure 3. ^{31}P NMR shift K versus temperature T for $Na_2CuP_2O_7$. The solid line is a fit to equation (4) over the temperature range 5 K $\leqslant T \leqslant$ 300 K, taking χ_{spin} for the HAF chain (equation (3)). In the inset we have displayed the data on a logarithmic scale in order to show the deviation of experimental data from the theory around the broad maximum region.

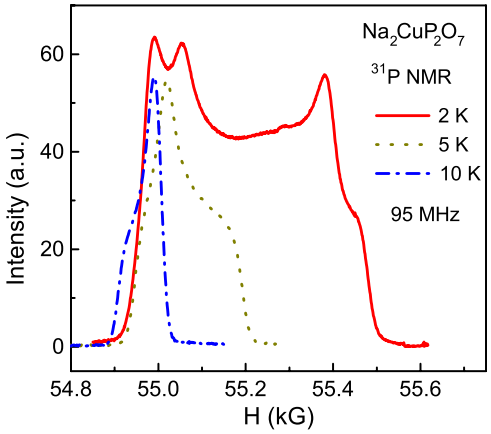

Figure 4. Low T field sweep ^{31}P NMR spectra for $Na_2CuP_2O_7$ are shown at different temperatures T around 5 K. This also shows the sudden change in linewidth and the appearance of several distinct peaks.

The magnetic susceptibility $\chi(T)$ $(=M/H)$ of $Na_2CuP_2O_7$ was measured as a function of temperature in an applied field of 5 kG (figure 5). The amount of ferromagnetic impurity present in our sample was estimated from the intercept of M versus H isotherms at various temperatures and was found to be 19 ppm of ferromagnetic Fe^{3+} ions. The data in figure 5 have been corrected for these ferromagnetic impurities. As shown in the figure, $\chi(T)$ exhibits a broad maximum at 20 K, indicative of low dimensional magnetic interactions. With a further decrease in temperature, the susceptibility increases in a Curie–Weiss manner. This possibly comes from defects and extrinsic paramagnetic impurities present in the samples. No obvious features associated with LRO are seen for 1.8 K $\leqslant T \leqslant$ 400 K.

The broad maximum in $\chi(T)$ at 20 K could be reproduced by assuming that

$$\chi = \chi_0 + \frac{C}{T+\theta} + \chi_{spin}(T) \tag{5}$$

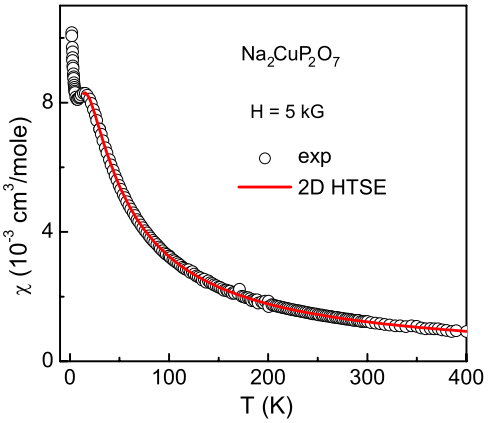

Figure 5. Magnetic susceptibility (M/H) versus temperature T measured at $H = 5$ kG for $Na_2CuP_2O_7$. The solid line is the best fit of the data to equation (5) in the 15 K $\leqslant T \leqslant$ 400 K range, taking χ_{spin} for the HAF square plane (equation (1)).

where $\chi_{spin}(T)$ is the uniform spin susceptibility for a $S = 1/2$ 2D HAF system obtained from equation (1). χ_0 is temperature independent and consists of diamagnetism of the core electron shells (χ_{core}) and Van Vleck paramagnetism (χ_{vv}) of the open shells of the Cu^{2+} ions present in the sample. The Curie–Weiss contribution is $\frac{C}{T+\theta}$ (where $C = \frac{Ng^2\mu_B^2 S(S+1)}{3k_B}$) due to paramagnetic species in the sample. The parameters were determined by fitting our experimental $\chi(T)$ data to equation (4) in the high temperature regime 15 K $\leqslant T \leqslant$ 400 K. The parameters extracted are $\chi_0 = (-7\pm2)\times10^{-5}$ cm^3 mol^{-1}, $C = (13\pm3)\times10^{-3}$ cm^3 K mol^{-1}, $\theta = 1.7$ K, $\frac{J}{k_B} = 18 \pm 2$ K, and $g = 2.07$. Adding the core diamagnetic susceptibilities for the individual ions [21] ($Na^{1+} = -5\times10^{-6}$ cm^3 mol^{-1}, $Cu^{2+} = -11\times10^{-6}$ cm^3 mol^{-1}, $P^{5+} = -1\times10^{-6}$ cm^3 mol^{-1}, $O^{2-} = -12\times10^{-6}$ cm^3 mol^{-1}), the total χ_{core} was calculated to be -1.07×10^{-4} cm^3 mol^{-1}. The Van Vleck paramagnetic susceptibility estimated by subtracting χ_{core} from χ_0 is about 3.7×10^{-5} cm^3 mol^{-1}, which is comparable to that found for Sr_2CuO_3 ($\sim3.4\times10^{-5}$ cm^3 mol^{-1}) [11]. The Curie contributions present in the sample correspond to a defect spin concentration of 3.5% assuming defect spin $S = 1/2$.

Further, we did heat capacity measurements on $Na_2CuP_2O_7$ to look for signs of any anomalies at low temperature, signalling a magnetic transition. As seen in the data (figure 6), no sharp peaks are visible, which seems to rule out LRO. However, a look at the derivative of the specific heat as a function of temperature (see the inset of figure 6) clearly shows a local maximum at about 7 K and a local minimum around 10 K. This suggests that the specific heat has an anomaly/peak between 7 and 10 K.[3] In the 2D HAF model, a broad maximum in the heat capacity is expected at about $T = 0.58J/k_B$ [18] (i.e. at about 10 K in the present case), whereas in the 1D HAF model, a broad maximum is expected at about $T = 0.48J/k_B$ [22] (i.e. at about 16 K in the present case). This further suggests the applicability of the 2D HAF model in the present case.

[3] This temperature range is not low enough for the 'T^3-approximation' of the lattice heat capacity to be valid. We tried to determine the lattice contribution to the specific heat by fitting the high temperature data (say, between 40 and 70 K, where the magnetic contribution may be expected to be negligible) to the exact expression of the Debye model. However, this fit (not shown) deviated significantly from the data when extrapolated to higher and lower temperatures. Considering larger ranges of temperature for the fit required us to use a temperature dependent (we tried a second order polynomial form with coefficients as fitting parameters) Debye temperature. This too did not appear to be helpful in reliably extracting the magnetic contribution at low temperatures (below 15 K).

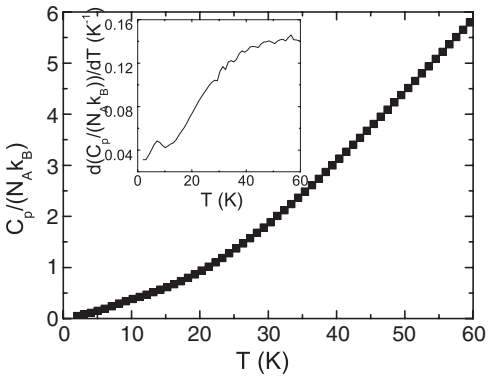

Figure 6. Normalized specific heat $C_p/(N_A k_B)$ of $Na_2CuP_2O_7$ is displayed as a function of temperature T. The inset has $d[C_p/(N_A k_B)]/dT$ as a function of T showing an anomaly around 10 K.

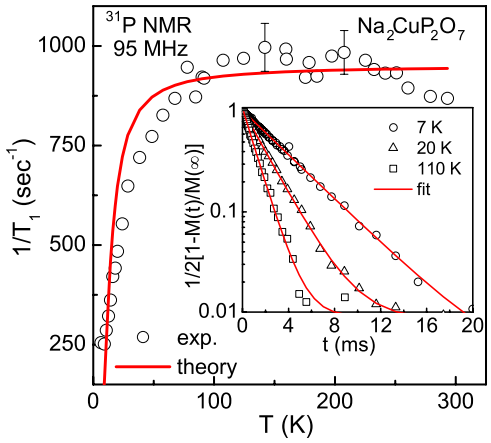

Figure 7. The ^{31}P nuclear spin–lattice relaxation rate $1/T_1$ versus temperature T for $Na_2CuP_2O_7$. The open circles are our experimental results and the solid line represents the simulated curve of equation (7). In the inset, the magnetization recoveries are plotted as a function of pulse separation t and the solid line is an exponential fit to equation (6).

The time dependence of the longitudinal nuclear magnetization $M(t)$ for ^{31}P at three different temperatures is shown in the inset of figure 7. For a spin-1/2 nucleus this recovery is expected to follow a single exponential behaviour

$$\frac{M(\infty) - M(t)}{M(\infty)} = A \exp\left(-\frac{t}{T_1}\right) + C. \tag{6}$$

Our experimental data show good single exponential behaviour over two decades. The spin–lattice relaxation rate $1/T_1$ was extracted from the fitting of the experimental data at various temperatures (down to 5 K) to equation (6). Due to the large line broadening we could not saturate the nuclear magnetization below 5 K and hence could not extract reliable $1/T_1$ data below this temperature. The temperature dependence of the ^{31}P nuclear spin–lattice relaxation rate thus obtained is presented in figure 7. With decrease in temperature, it decreases monotonically. For $S = 1/2$ 2D square lattice, a high temperature series expansion for $1/T_1$

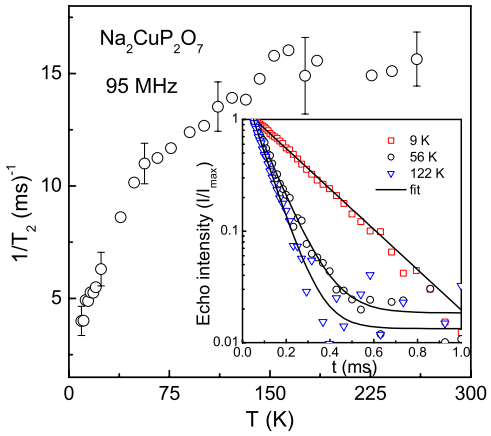

Figure 8. The ^{31}P spin–spin relaxation rate $1/T_2$ is plotted as a function of temperature T. In the inset, spin-echo decays are plotted as a function of t at three different temperatures for $Na_2CuP_2O_7$. The solid lines show the fitting to an exponential function (equation (8)).

was given by Moriya [23]; it has the form

$$1/T_1 = \frac{1}{T_{1\infty}\,(1 + J/(4k_BT))^{1/2} \exp\left[(J/(2k_BT))^2(1 + J/(4k_BT))\right]} \tag{7}$$

where, $\frac{1}{T_{1\infty}} = (\frac{A_{th}^2}{\hbar^2})(\frac{\sqrt{\pi}\hbar k_B}{4J})$, taken from [24]. Here, $A_{th} = 2A\hbar\gamma$ where A is the total hyperfine coupling obtained from the experiment. In Moriya's expression a term of the order of $(J/k_BT)^2$ occurs in the prefactor and has a negligible effect and hence is not included in equation (7). Using equation (7) and the relevant A and J/k_B values obtained from the fit of the NMR shift to the 2D model, we simulated the theoretical curve for $Na_2CuP_2O_7$ and it is plotted with our experimental data in figure 7. Clearly, at high temperatures ($T \geqslant 25$ K), the experimental data agree reasonably well with the simulated curve. In the case of a $S = 1/2$ 1D HAF chain model, $1/T_1$ is expected to be temperature independent at low temperatures ($T \ll J/k_B$) due to a dominant contribution from the fluctuations of the staggered susceptibility of the 1D chain. We are unable to probe this region of temperature due to the large broadening of our NMR spectra seen there. At higher temperatures, from fluctuations of the uniform susceptibility of the 1D chain, one expects a linear variation of $1/T_1$ with temperature. This should eventually saturate at even higher temperatures when the spin susceptibility becomes Curie-like. Qualitatively speaking, the observed $1/T_1$ data could be explained on the above basis. However, an analytical expression for the temperature dependence of $1/T_1$ is not available in the temperature regime of our experiment and hence no curve fit is shown in the figure.

The spin–spin relaxation was measured as a function of separation time t between $\pi/2$ and π pulses by monitoring the decay of the transverse magnetization. $1/T_2$ at different temperatures was obtained by fitting the spin-echo decay to the following equation:

$$M\,(2t) = M_0 \exp\left[-2\left(\frac{t}{T_2}\right)\right] + C. \tag{8}$$

The inset of figure 8 shows the spin-echo decays for different temperatures. The extracted spin–spin relaxation rates $1/T_2$ are plotted as a function of temperature in figure 7. It can be seen that below about 55 K, the spin–spin relaxation rate $1/T_2$ falls sharply towards low temperatures. No indication of 3D LRO was found down to 6 K. The origin of this temperature dependence $1/T_2$ is not clear yet.

5. Conclusion

Our ^{31}P NMR shift and susceptibility data fitted reasonably well to the high temperature series expansion for 2D HAF model whereas the fitting to the 1D model was not as good, especially in the $T \leqslant 25$ K regime. From the ^{31}P NMR shift analysis, the J/k_B value was estimated to be about 18 ± 2 K. The large broadening of the ^{31}P NMR spectra at $T \leqslant 5$ K points towards a transition. However, no evidence of magnetic LRO was found in susceptibility and heat capacity measurements down to 2 K. Further experiments are required to really understand the detailed nature of this transition. ^{31}P NMR $1/T_1$ data show a good agreement with the theory of the 2D HAF square lattice. The results reported in this paper thus suggest a variety of experiments and a need for a better theoretical understanding of quasi-low dimensional Heisenberg antiferromagnets.

Acknowledgments

We would like to kindly acknowledge D Vieweg for SQUID measurements and Th Wiedmann for heat capacity measurements. One of us (AVM) would like to thank the Alexander von Humboldt foundation for financial support for a stay at Augsburg. This work was supported by the BMBF via VDI/EKM, FKZ 13N6917-A and by the Deutsche Forschungsgemeinschaft (DFG) through the Sonderforschungsbereich SFB 484 (Augsburg).

References

[1] Mermin N D and Wagner H 1966 *Phys. Rev. Lett.* **17** 1133
[2] Affleck I, Kennedy T, Lieb E H and Tasaki H 1988 *Commun. Math. Phys.* **115** 477
[3] Neves J and Perez F 1986 *Phys. Lett.* A **144** 331
[4] Kennedy T, Lieb E H and Shastry B S 1988 *J. Stat. Phys.* **53** 1019
[5] Singh R R P, Gelfand M P and Huse D A 1988 *Phys. Rev. Lett.* **61** 2484
[6] Aeppli G, Hayden S M, Mook H A, Fisk Z, Cheong S-W, Rytz D, Remeika J P, Espinosa G P and Cooper A S 1989 *Phys. Rev. Lett.* **62** 2052
[7] Singh R R P, Fleury P A, Lyons K B and Sulewski P E 1989 *Phys. Rev. Lett.* **62** 2736
[8] Wu M K, Ashburn J R, Torng C J, Hor P H, Meng R L, Gao L, Huang Z J, Wang Y Q and Chu C W 1987 *Phys. Rev. Lett.* **58** 908
[9] Chakhalian J, Kiefl R F, Miller R, Dunsiger S R, Morris G, Kreitzman S, MacFarlane W A, Sonier J, Eggert S, Affleck I and Yamada I 2003 *Physica* B **326** 422
[10] Hutchings M T, Samuelsen E J, Shirane G and Hirakawa K 1969 *Phys. Rev.* **188** 919
[11] Motoyama N, Eisaki H and Uchida S 1996 *Phys. Rev. Lett.* **76** 3212
[12] Nath R, Mahajan A V, Büttgen N, Kegler C and Loidl A 2005 *Phys. Rev.* B **71** 174436
[13] Etheredge K M S and Hwu S 1995 *Inorg. Chem.* **34** 1495
[14] Erragh F, Boukhari A, Abraham F and Elouadi B 1995 *J. Solid State Chem.* **120** 23
[15] Rushbrooke G S and Wood P J 1958 *Mol. Phys.* **1** 257
[16] Johnston D C 1997 *Handbook of Magnetic Materials* ed K H J Buschow (Amsterdam: Elsevier)
[17] Takahashi M 1989 *Phys. Rev.* B **40** 2494
[18] Makivic M S and Ding H-Q 1991 *Phys. Rev.* B **43** 3562
[19] Bonner J C and Fisher M E 1964 *Phys. Rev.* **135** A640
[20] Estes W E, Gavel D P and Hodgson D 1978 *Inorg. Chem.* **17** 1415
[21] Selwood P W 1956 *Magnetochemistry* 2nd revised edn (New York: Interscience)
[22] Johnston D C, Kremer R K, Troyer M, Wang X, Klümper A, Bud'ko S L, Panchula A F and Canfield P C 2000 *Phys. Rev.* B **61** 9558
[23] Moriya T 1956 *Prog. Theor. Phys.* **16** 23
[24] Chakravarty S and Orbach R 1990 *Phys. Rev. Lett.* **64** 224